**Annales
Geophysicae**

Compressional wave events in the dawn plasma sheet observed by Interball-1

O. Verkhoglyadova[1], A. Agapitov[1], A. Andrushchenko[2], V. Ivchenko[1], S. Romanov[3], Yu. Yermolaev[3]

[1] Department of Astronomy and Space Physics, Taras Shevchenko Kiev University, Vladimirskaya 64, Kiev 252017, Ukraine
e-mail: verkh@astrophys.ups.kiev.ua
[2] Space Research Institute NASU and NSAU, Kiev, Ukraine
[3] Space Research Institute, Profsoyuznaja, 84/32, Moscow 117810, Russia

Abstract. Compressional waves with periods greater than 2 min (about 10–30 min) at low geomagnetic latitudes, namely compressional Pc5 waves, are studied. The data set obtained with magnetometer MIF-M and plasma analyzer instrument CORALL on board the Interball-1 are analyzed. Measurements performed in October 1995 and October 1996 in the dawn plasma sheet at $-30\,R_E \le X_{GSM}$ and $|Z_{GSM}| \le 10\,R_E$ are considered. Anti-phase variations of magnetic field and ion plasma pressures are analyzed by searching for morphological similarities in the two time series. It is found that longitudinal and transverse magnetic field variations with respect to the background magnetic field are of the same order of magnitude. Plasma velocities are processed for each time period of the local dissimilarity in the pressure time series. Velocity disturbances occur mainly transversely to the local field line. The data reveal the rotation of the velocity vector. Because of the field line curvature, there is no fixed position of the rotational plane in the space. These vortices are localized in the regions of anti-phase variations of the magnetic field and plasma pressures, and the vortical flows are associated with the compressional Pc5 wave process. A theoretical model is proposed to explain the main features of the nonlinear wave processes. Our main goal is to study coupling of drift Alfven wave and magnetosonic wave in a warm inhomogeneous plasma. A vortex is the partial solution of the set of the equations when the compression is neglected. A compression effect gives rise to a nonlinear soliton-like solution.

Key words. Magnetosphere physics (magnetotail) ·
Space plasma physics (kinetic and MHD theory;
non-linear phenomena)

Introduction

Concurrent variations of the magnetic field pressure and plasma thermal pressure with periods greater than 2 min (about 10–30 min) at low geomagnetic latitudes, namely compressional Pc5 waves, have been variously studied based on the data set obtained with OGO 5 (Kokubun *et al.*, 1977), ATS 6 (Su *et al.*, 1977), ATS 1 (Barfield and McPerron, 1978), GOES 2, 3 (Barfield and Lin, 1983), GEOS 2 (Walker *et al.*, 1982) and AMPTE (Bauer *et al.*, 1995). It should be noted that the measurements performed at the geostationary orbit with two satellites GOES 2, 3 (Takahashi *et al.*, 1985) and four satellites (Takahashi *et al.*, 1987) revealed the standing structure of the compressional Pc5 wave along the geomagnetic field line (Takahashi, 1988; Takahashi *et al.*, 1990). Extensive classification of the ULF wave events in the Pc3–5 frequency range detected under the magnetopause was carried out by Anderson *et al.* (1990). The main features of the ULF events are described in the literature cited as follows:

1. Coincidence of the mean period of quasi-sinusoidal signal with the typical periods of Pc3–5
2. Anti-phase variations of ion plasma pressure and magnetic field pressure
3. Localization in the low-latitude flank sectors
4. Relatively high values of plasma $\beta \sim 1$
5. Comparable oscillations of longitudinal (compressional) and transverse magnetic field components with respect to the background magnetic field
6. Association with the geomagnetic storm activity

Except for analysis of ISEE 1/2 data (Zhu and Kivelson, 1991, 1994), studies of the compressional Pc5 waves were performed using data obtained relatively close to the Earth at the geocentric distances of less than or about 10 Earth radii. The goal of our analysis is to study similar wave events in the middle tail, i.e. at geocentric distances of about 20 Earth radii. Because of different

physical conditions in these regions, excitation mechanisms of the waves should be also different.

Several mechanisms have been considered to explain the excitation of compressional ULF events in a warm inhomogeneous plasma environment with $\beta \leq 1$ at the low-latitude inner plasma sheet and in the vicinity of the ring current region. One of them applied to the waves with large azimuth numbers (m $\sim 10^2$) was proposed in a number of papers (Chen and Hasegawa, 1991, 1994; Chan et al., 1994) and studied in terms of the reduced gyrokinetic theory. The local instabilities due to energetic particle fluxes in inhomogeneous core plasma with anisotropic velocity distribution are assumed to be the main wave excitation mechanism. Thus, coupled drift-Alfven ballooning mirror modes were considered to explain the observed phenomena (Chen and Hasegawa, 1991; Chan et al., 1994). Alternative excitation mechanism of the waves with both compressional and transverse components taking into account pressure anisotropy and magnetic field curvature-pressure gradient factors was proposed in the papers by Cheng (1991, 1994b) and Cheng and Qian (1994a). Internal (local) instabilities under realistic plasma conditions at closed field lines are suggested as a probable excitation mechanism in all these models. Energetic particle fluxes originated in the ring current region can produce wave excitation. The mechanism that could be responsible for excitation of similar compressional waves measured at the geocentric distances of about 20 Earth radii requires further study.

Vortex events were investigated in the dawn plasma sheet using the ISEE-1, 2 data (see Hones et al., 1978; Hones et al., 1981; Saunders et al., 1981; Hones et al., 1983; Saunders et al., 1983a, b). Distinct plasma rotations were observed during intervals of 20 min and velocity ranged within 30 and 300 km/s. Spatial scales of about 5 Earth radii were detected. Those results were interpreted as evidence for a convective vortex street induced by the Kelvin-Helmholtz instability. However, the vortical flows were found to be associated with long-period geomagnetic pulsations. The nature of this connection is still poorly understood.

The present study is based on the experimental data obtained with the Interball-1 instruments. To study properties of compressional wave events in the dawn plasma sheet, the authors provided an analysis of plasma and magnetic field measurements in the middle tail of the Earth magnetosphere for selected time intervals. Reliable identification of the anti-phase variations of the plasma and magnetic field pressures, and possible association with vortex flows in the same region were of great interest. A theoretical model is considered to explain the main features of the nonlinear wave processes. The main goal of such an analysis is to study the coupling of the drift Alfven wave and magnetosonic wave.

Data analysis

The measurements obtained in October 1995 and October 1996 when Interball-1 probe was situated in the low-latitude dawn flank of the magnetosphere were selected. The data obtained with the magnetometer MIF-M (Klimov et al., 1997) and the plasma analyzer instrument CORALL (Yermolaev et al., 1997) were analyzed. This study is mainly based on the key parameters, i.e. the data averaged over 2-min intervals. The region studied was limited by the conditions $X \leq -5$ and $Z \leq 10$, with coordinates taken in the GSM-system in the Earth's radii. Then we selected the time intervals for which the data from the both instruments were available. Using the plasma regime identification criteria for data selection (Eastman et al., 1997; Christon et al., 1997) we excluded the lobe region crossings from the study. Only the data obtained in the plasma sheet and boundary layers were considered. Ion temperatures and plasma densities vary within $10^2 - 10^3$ eV and 0.1–10 cm^{-3} respectively. Probe positions with 1 h time resolution of the selected time intervals are shown in Fig. 1. Magnetopause position is evaluated according to the model presented by Sibeck et al. (1991). The measurements obtained far enough from the magnetopause are analyzed. For the time intervals under study the mean distance of the probe from the magnetopause was about 6 Earth radii and the most of the measurements were obtained at distances about 4 Earth radii from it. Time intervals and corresponding probe coordinates (in the Earth radii) are listed in Table 1, where 'dd' is the day and 'hh' is the hour (in UT). The indices 1 and 2 denote values attributed to initial and final positions of the spacecraft at selected time intervals, respectively. Mean values of the activity index D_{st} provided by the WDC-B are presented.

Firstly, the compressional wave events were identified by comparing anti-phase variations of the magnetic pressure and plasma thermal pressure, and thus corresponding time intervals of the events were selected. These variations are typical for the magnetosonic-type and mirror disturbances in homogeneous plasma. Then, low-frequency waves have both Alfven-type and magnetosonic-type properties in inhomogeneous plasma with curvilinear background magnetic field (Mikhaylovskiy, 1991). Thus, these waves have comparable variations of compressional and transverse magnetic field components with respect to the background magnetic field. Some events are shown in Fig. 2a–d. The magnetic field pressure and plasma thermal pressure time series are presented there. The data without linear trend processed with a digital filter are also shown.

Special methods and software were developed to select sub-intervals with distinct anti-phase variations of the pressure data identifying the compressional wave events. These variations manifest themselves by dissimilarities in the pressure data for selected time intervals. Such a method is based partly on some approaches used for searching of local similarities in DNA strings (Huang and Miller, 1991; Huang and Waterman, 1992). Simultaneously, it is necessary to notice that these approaches can not be applied directly to our study since they were used for data sets where the corrupting influence of noise was not considered.
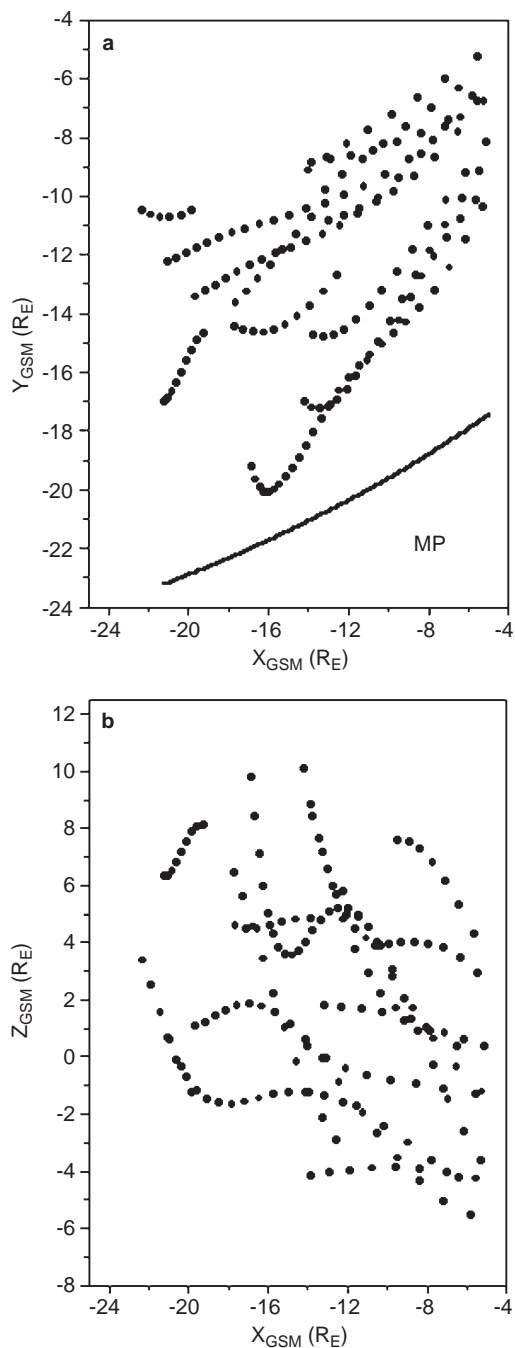
Fig. 1a, b. Probe positions in the dawn flank of the magnetosphere in selected time intervals: **a** projection into XY plane (model magnetopause (Sibeck *et al.*, 1991) is shown); **b** projection into XZ plane

However, our data are characterized by a relatively large level of noise. This noise includes both instrumental noise and other disturbances which are beyond our study. So, time segments with anti-phase-variations of the pressures (dissimilarity segments) and time segments with in-phase variations of the pressures (similarity or noisy segments) occur intermittently in the studied time intervals. These noisy segments are considered as "false alarms". Note that the term "false alarm" is widely used in the field of time series segmentation, target detection etc. It is obvious that total length of all false alarm

segments cannot be too large with respect to the length of the remaining segments with dissimilarities. We introduce the zero statistical hypothesis about the random character of an interval. Then Mann-Whitney rank-sum statistics were used to verify and to reject the hypothesis (Basseville and Beveniste, 1986). We supposed that the dissimilarity segment length had to be larger than that of the false alarm segment. The dynamic programming approach was used to solve the respective global optimization problem. Result of application of the selection procedure to two random data series is presented in Fig. 3. The dissimilarity segment is shown by the bottom line. The maximum probability of "false alarms" in the data segment, i.e. ratio of 'bad points' to the 'good points', is not higher than 0.21.

Thus, the time sub-intervals with durations more than 20 min and with local dissimilarities in the two time series with the false alarm probability of about 0.21 are used. The magnitude of cross-correlation coefficient for the pressure data estimated for the intervals listed in Table 1 is about 0.1–0.5. In the time series 'good' segments with distinct anti-correlation occur intermittently with noisy segments. This effect explains the relatively low value of the coefficient. In contrast, the magnitude of the cross-correlation coefficient for selected sub-intervals reaches 0.7–0.99. Some of the sub-intervals with low-frequency anti-phase variations are shown in Fig. 2a–d by the bottom lines. Compressional events were selected for both disturbed and medium activity conditions (see Table 1). It should be noted that for several selected time intervals in the measurements obtained in the dusk flank in December 1995 and December 1996, compressional wave events are not found. This result points to possible dawn-dusk asymmetry of the wave process.

To study spectra properties polynomial filters with high-frequency cut-off and improved characteristics in the low-frequency region were used. Results revealed some correspondence between the frequency peaks in the magnetic field and plasma pressure data. The synthetic spectra of a time series constructed by joining plasma and magnetic pressure data corresponding to local dissimilarities found in October 1995 data is shown in Fig. 4. The local dissimilarity interval with minimum duration corresponds to an arrowed frequency. The wave periods corresponding to spectra maxima of the pressures are about 10–20 min. These values are different for various time intervals. It is assumed that the fact can be explained by distinctions of plasma parameters for different space regions.

The second step of our study was to extract the background magnetospheric field from the data records. The determination of the direction of the magnetic field disturbances with respect to the local field line was made. For this purpose, the averaging of the magnetic field data by a filter over 1 h time intervals was performed. Averaged field values are shown in Fig. 5a, b by lines. Points indicate the experimental data with 2 min resolution. Variations of compressional and transverse magnetic field components are of the same order of magnitude. They are presented in Fig. 6a, b, where solid

Table 1. Time intervals selected for the study. Coordinates are presented in the GSM-system in the Earth's radii, dd is the day and hh is the hour (in UT). The indices 1 and 2 denote the values attributed to the initial and final positions of the spacecraft, respectively

N	dd_1	hh_1	X_1	Y_1	Z_1	dd_2	hh_2	X_2	Y_2	Z_2	D_{st}
October 1995											
1	2	06	−9.4	−14.3	7.6	2	12	−5.6	−10.2	4.3	−05
2	5	17	−14.2	−17.0	10.1	6	08	−5.4	−9.2	2.9	−51
3	9	16	−13.7	−14.7	7.2	10	04	−5.1	−8.2	0.4	−51
4	17	11	−12.9	−10.9	6.6	17	19	−5.2	−6.8	−1.2	−25
5	21	00	−17.6	−13.6	4.6	21	06	−14	−10.8	4.8	−51
6	25	03	−13.2	−9.8	1.8	25	09	−6.4	−6.3	0.3	−43
7	28	22	−13.9	−9.1	0.4	29	05	−5.5	−5.3	−1.3	−09
October 1996											
1	3	17	−16.8	−19.3	9.7	4	18	−5.3	−10.4	−3.6	−08
2	15	0	−21.2	−17.0	6.3	15	08	−19.2	−14.7	8.1	−22
3	15	12	−17.7	−14.5	6.5	15	21	−12.5	−12.7	−2.9	−13
4	23	3	−19.2	−13.2	1.2	23	19	−5.8	−6.6	−5.6	−63
5	26	20	−21.0	−12.2	0.6	27	14	−6.4	−7.3	−4.2	−16
6	30	14	−22.3	−10.5	3.4	30	19	−19.8	−10.5	−1.3	−27
7	31	3	−13.8	−8.9	−4.2	31	10	−5.5	−6.8	−4.3	−31

lines correspond to the compressional component and dashed lines correspond to the transverse component. The power spectra for each component reflect features of both magnetic field and plasma pressure oscillations. Therefore the process can be considered as a result of coupling between Alfven-type wave and magnetosonic-type wave.

An alternate procedure of magnetosphere magnetic field evaluation is based on the updated empirical model by Tsyganenko (1995), and Tsyganenko and Stern (1996). The last version of the model contains new representation of tail and ring currents and parametri-zation by D_{st} index. Solar wind dynamic pressure P_{dyn}, interplanetary magnetic field components B_y and B_z, D_{st} index are used as input parameters for magnetosphere magnetic field simulations at the positions of Interball-1. Current geodipole tilt angle is determined using the program package GEOPACK updated by N. A. Tsyganenko and M. Peredo in 1996. The solar wind data obtained on board the WIND spacecraft were taken through the ISTP key parameter program. The time delay required for solar wind flow to reach the subsolar magnetopause point from the WIND position is taken into account. Such time delays calculated in the simplest way are from 30 to 50 min for the time intervals under study. The model shows a good agreement with the average value of the measured magnetic field for days with medium D_{st}, but experimental values are somewhat higher than those of the model for quiet days just after unusually active periods. Several model field values (indicated by crosses) are presented for comparison in Fig. 5. According to the simulation the decrease in D_{st} index leads to the increase of B_y and B_z background field components at the flanks. With energy being stored in the magnetosphere, the background field is assumed to be disturbed for a prolonged time interval. This effect is not taken into account in the empirical model. Simulation results are arguments in favour of connection of background magnetic field enhancement with the ring current disturbances during active geo-magnetic periods. Such a discrepancy between the model and mean experimental values may be also explained by the crude evaluation of the time delay. To find a reliable time lag, a correlation analysis between solar wind and magnetosphere parameters in the region under study should be made. Therefore, this method of evaluation of the field components was rejected in the current study.

Under the third stage of the study, connection of the compressional waves with vortical flows is considered. According to theory, vortices and vortex tubes are typical features of nonlinear drift Alfven waves. The vortices are assumed here to deal with the low-frequency anti-phase variations of the pressures. To verify the assumption, time intervals with enough number of 'good points', i.e. time sub-intervals with relatively low level of noise are studied. Plasma velocities are processed for each time interval during which the local dissimilarity in the pressure time series, i.e. distinct anti-phase behav-iour in the time series, is found. Distribution of angles between field line and the velocity vectors are presented in Fig. 7. Velocity disturbances occur predominantly in the orthogonal direction to the local field line. The velocity data reveal the vector rotations in the studying time intervals. Velocity hodographs in the plane (*XY*) of the GSM coordinate system are presented in Fig. 8. Application of the minimum variance method shows that there is no fixed position of the rotational plane in the space. This plane can change its orientation in a space because of the field line curvature.

Thus, it is assumed that the vortical flows are connected with the compressional wave processes. It should be noted that these vortices are localized in the regions of anti-phase variations of the magnetic field and plasma pressures. To support this statement we note that the vortices and compressional wave events are detected at the same time intervals (compare Figs. 2 and 8).
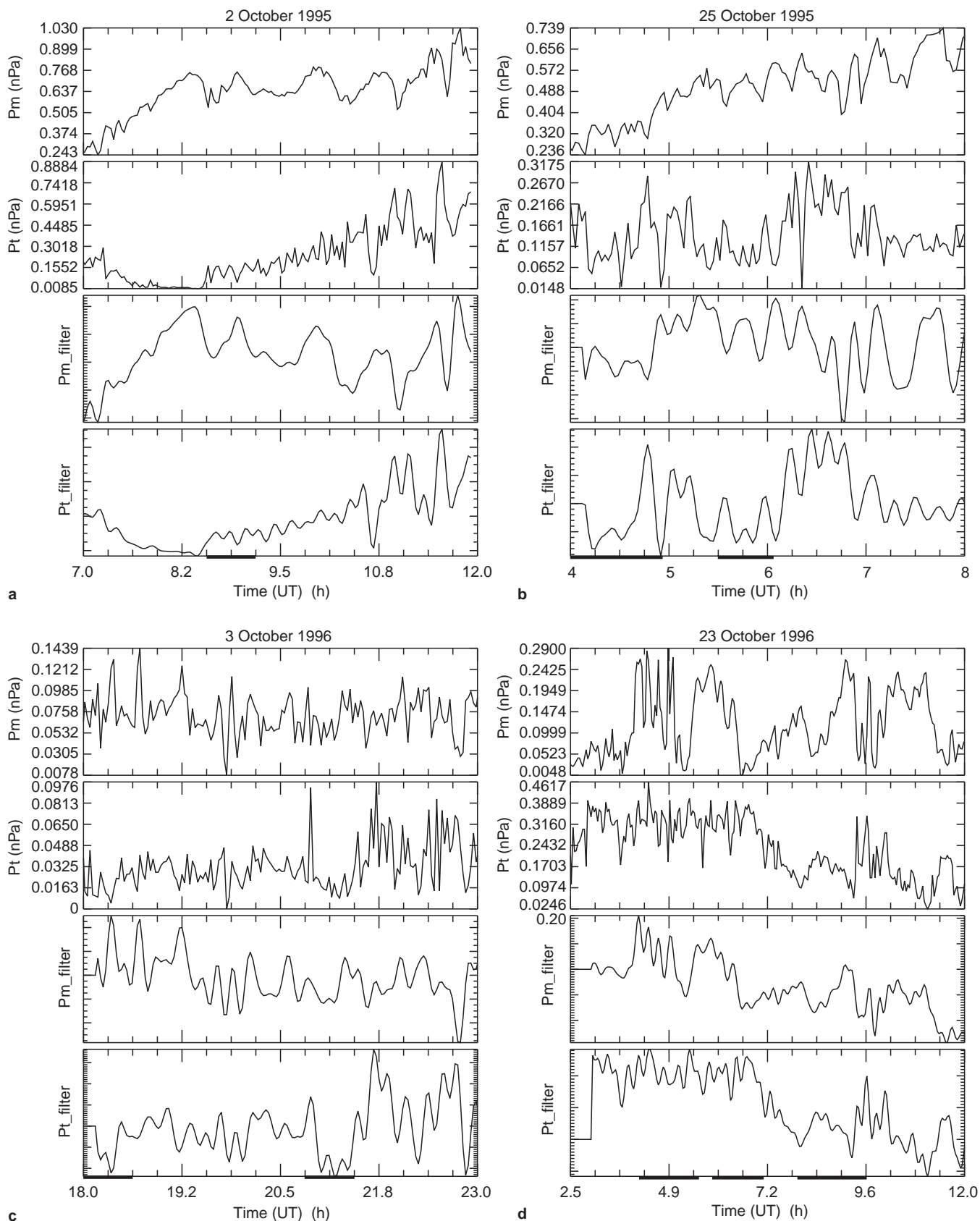
Fig. 2a–d. Magnetic pressure and plasma pressure (*upper panels*) are presented for the time intervals: **a** from 07:00 UT to 12:00 UT 2 October 1995; **b** from 04:00 UT to 8:00 UT 25 October 1995; **c** from 18:00 UT to 23:00 UT 3 October 1996; **d** from 03:00 UT to 11:00 UT 23 October 1996. The data without linear trend processed with a digital filter are shown in the *lower panels*
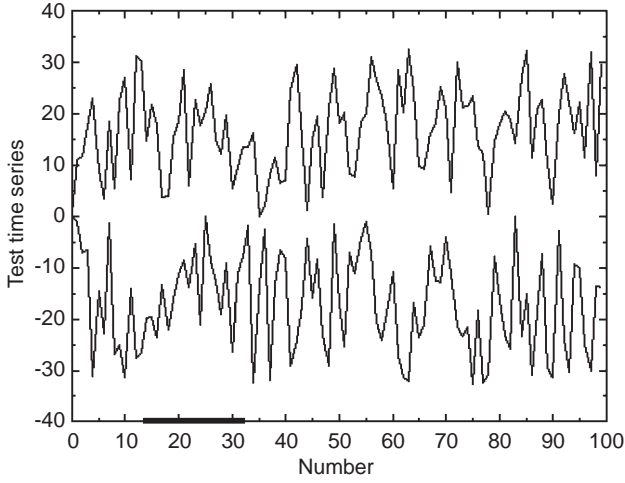
Fig. 3. Example of two random data series with selected dissimilarity segment (shown by the *lower line*)

Model of the nonlinear compressional waves

The low-frequency large-scale phenomena accompanied by large-amplitude compression effects and rotation of the ion velocity vectors were discovered. The former feature represents the fast magnetosonic waves causing the strongest compression effect in the warm plasma with $\beta \leq 1$. The latter feature may be explained in terms of the drift Alfven vortices in inhomogeneous plasma. Several theoretical models were developed applying formalism of nonlinear drift Alfven waves to treat the ionosphere and magnetosphere vortical events (Petviashvili and Pokhotelov, 1989; Chmyrev *et al.*, 1988). The wave events detected far enough from the model magnetopause were studied (see Fig. 1). The mean distance of the probe from the model magnetopause was about 6 Earth radii. Thus excitation of these waves due to the Kelvin-Helmholtz instability is not considered.
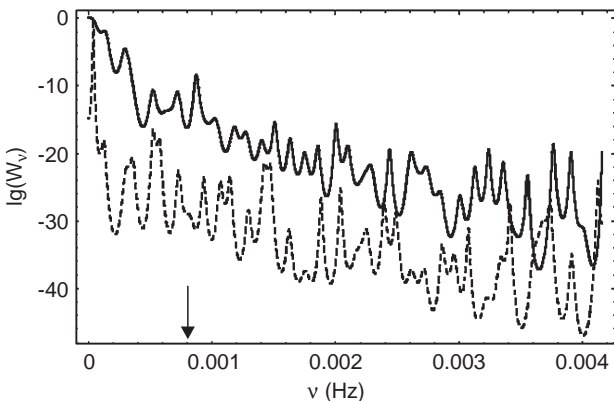

Fig. 4. Wave spectra of the time series constructed by joining plasma and magnetic pressure data corresponding to local dissimilarities found in October 1995 data
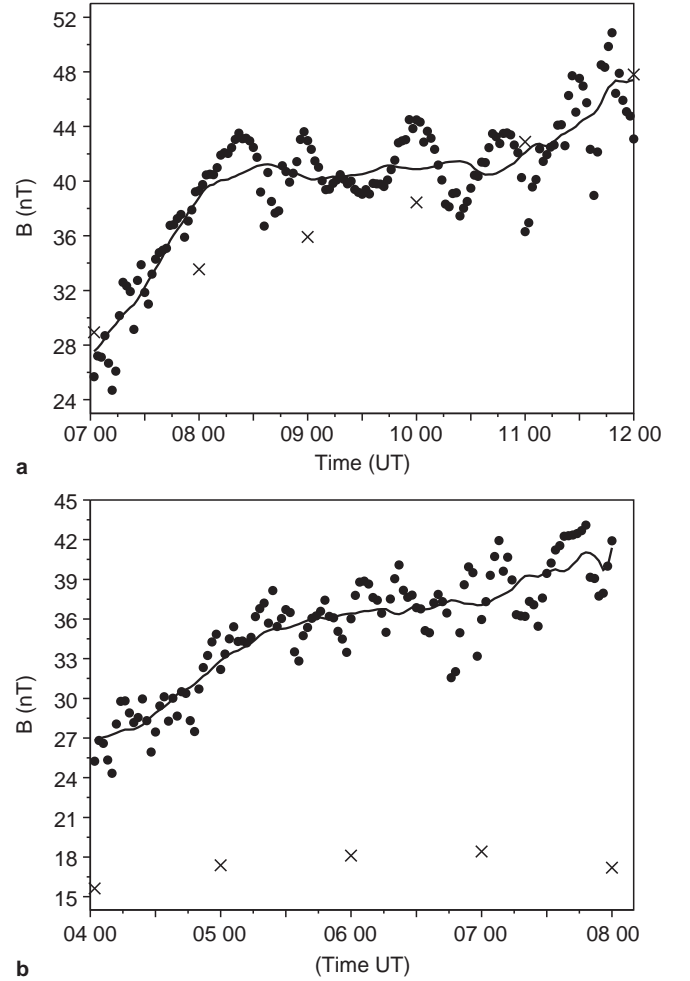

Fig. 5a, b. Averaged values of the magnetic field magnitude (*solid lines*) and corresponding experimental data with 2 min resolution (*points*) are presented for time intervals from 07:00 UT to 12:00 UT 2 October, 1995 and of from 04:00 UT to 8:00 UT 25 October, 1995

Alfven vortices in the dawn plasma sheet with taking into account variations of the magnetic field along the field line were considered. Thus, the coupling of the drift Alfven wave with the fast magnetosonic wave, that occur in warm plasma environment, was included in the consideration.

Following the standard approach to the problem, large-scale and slow wave processes ($\omega \ll \omega_{Bi}, \lambda \gg \frac{V_{Ti}}{\omega_{Bi}} = \rho_i$) in a plasma system which is inhomogeneous in X-direction was considered (see Fig. 9). Here ω_{Bi} is the ion gyrofrequency, and ρ_i is the ion gyroradius. The magnetic field variations are expressed using the parallel vector potential component and variation of the parallel magnetic field:

$$\vec{B} = \vec{B}_0 + \vec{B}_{\parallel} + \vec{B}_{\perp}, \quad \vec{B}_{\perp} = \left[\vec{\nabla} A_{\parallel}, \ \frac{\vec{B}_0}{\mathbf{B}_0} \right],$$

$$\left| \vec{B}_0 \right| > \left| \vec{B}_{\perp} \right| > \left| \vec{B}_{\parallel} \right| .$$

Here the square brackets denote vector product. The electric field variations take the form:
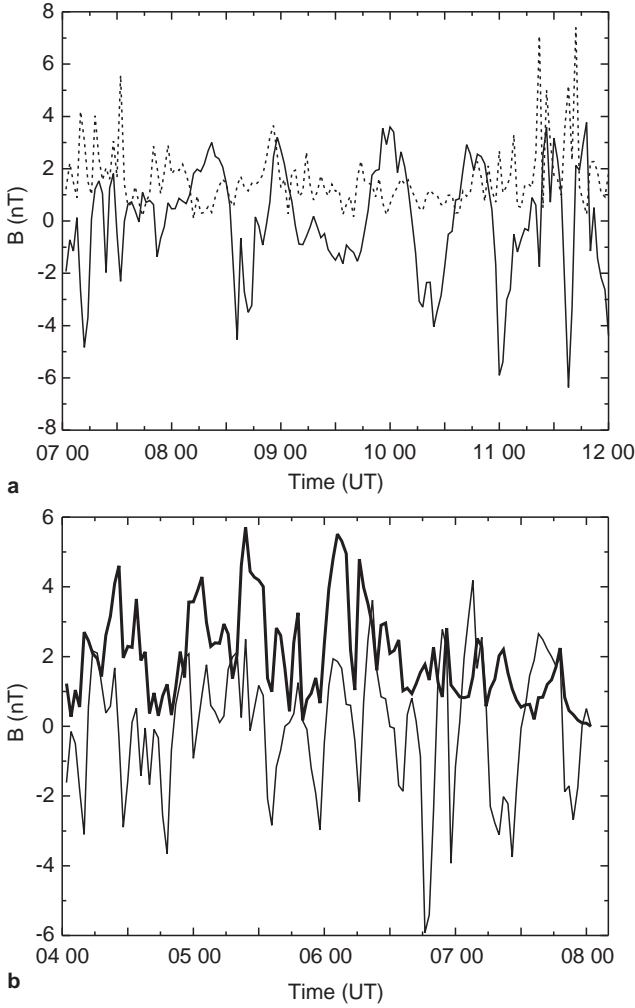
Fig. 6a, b. Magnetic field variations along and transversely to the background magnetic field for the same intervals as for Fig. 5. The *solid lines* correspond to compressional component and *dashed lines* correspond to transverse component

$$\vec{\mathbf{E}} = \vec{\mathbf{E}}_\perp + \vec{\mathbf{E}}_{||}, \quad \mathbf{E}_{||} = -\frac{\left(\vec{\mathbf{B}}_0 + \vec{\mathbf{B}}_{||}\right) \cdot \vec{\nabla}\phi}{\mathbf{B}_0} - \frac{1}{c}\frac{\partial \mathbf{A}_{||}}{\partial t},$$

$$\mathbf{E}_\perp = -\frac{\vec{\mathbf{B}}_\perp \cdot \vec{\nabla}\phi}{\mathbf{B}_0} \;,$$

where ϕ is the potential of the electric field. For low β-plasma in the framework of standard approach we consider $\lambda_\perp \ll \lambda_{||}$ and $\vec{\mathbf{V}} \approx \vec{\mathbf{V}}_\perp$. So, the wave propagates almost transversely to the local field line and $\mathbf{B}_{||} \to 0$. A basic nonlinear system of equations was derived for the Vlasov equation for ions averaged over the cyclotron rotation and for the equation of electron motion along the field line (Chmyrev et al., 1988). Partial solutions of the system are Alfven vortices and vortex chains.

In the case of finite β-plasma we include $\mathbf{B}_{||} \neq 0$. Thus magnetic field transverse variations relative to local field lines represent the Alfven-type waves and variations along the field line are connected with the magnetosonic-type waves. The equation for $\mathbf{B}_{||}$ was obtained from projection of the equation of electron motion into the plane which is transverse to the field line:

$$m_e \mathbf{n}\frac{\mathrm{d}}{\mathrm{d}t}\vec{\mathbf{V}}_\perp + e\mathbf{n}\vec{\mathbf{E}} + \vec{\nabla}_\perp \mathbf{p} + \frac{e\mathbf{n}}{c}\left[\vec{\mathbf{V}}, \vec{\mathbf{B}}\right]_\perp = 0 \;, \tag{1}$$

where $\mathbf{p}$ is the pressure and $\vec{\mathbf{V}}$ is the electron velocity. $\vec{\mathbf{V}}_\perp$ is determined by the electric drift velocity. In this drift approximation electric field transverse variations relative to the local field line are almost potential. The result takes the form:

$$\frac{\mathrm{d}}{\mathrm{d}t}\left(\varepsilon \Delta_\perp \phi - \mathbf{B}_{||}\right) = 0, \quad \varepsilon = \frac{m_e}{m_i} \ll 1,$$

$$\frac{\mathrm{d}}{\mathrm{d}t} = \frac{\partial}{\partial t} + \{\phi, ...\} \;, \tag{2}$$

where we use the dimensionless variables according to the paper by Chmyrev et al. (1988):

$$x, y \leftrightarrow x/\rho_s, \quad y/\rho_s, \quad t \leftrightarrow t \cdot \omega_{Bi}, \quad \phi \leftrightarrow e\phi/T_e,$$

$$z \leftrightarrow z\omega_{Bi}/\rho_s, \quad \mathbf{A} = \frac{e\mathbf{V}_A}{cT_{e0}} \cdot \mathbf{A}_{||}, \quad \mathbf{N} = \frac{\mathbf{n}_e}{\mathbf{n}_0} - 1,$$

$$\mathbf{P} + \frac{T_{i0}}{T_{e0}} = \frac{\mathbf{p}_i}{n_0 T_{e0}} \;,$$

and the Poisson brackets: $\{f, \varphi\} = \frac{\partial f}{\partial x} \cdot \frac{\partial \varphi}{\partial y} - \frac{\partial f}{\partial y} \cdot \frac{\partial \varphi}{\partial x}$.

Here we used Alfven velocity $\mathbf{V}_A$, particle number density $\mathbf{n}$ and the spatial scale $\rho_s = \frac{C_s}{\omega_{Bi}}$, where C_s – is the ion sound velocity. The form of the main system of equations remains unchanged (Petviashvili and Pokhotelov, 1985; Chmyrev et al., 1988):

$$\frac{\mathrm{d}}{\mathrm{d}t}\mathbf{P} = 0,$$

$$\frac{\mathrm{d}}{\mathrm{d}t}\mathbf{A} - \delta\frac{\partial}{\partial t}\mathbf{J} = \frac{\mathrm{d}}{\mathrm{d}z}(\mathbf{N} - \phi),$$

$$\mathbf{J} = \Delta_\perp \mathbf{A},$$

$$\frac{\mathrm{d}}{\mathrm{d}t}\mathbf{N} + \frac{\mathrm{d}}{\mathrm{d}z}\mathbf{J} = 0, \tag{3}$$

$$\frac{\mathrm{d}}{\mathrm{d}t}\Delta_\perp \phi = -\frac{\mathrm{d}}{\mathrm{d}z}\mathbf{J} - \vec{\mathbf{V}} \cdot \{\mathbf{P}, \vec{\mathbf{V}}_\perp \phi\},$$

$$\frac{\mathrm{d}}{\mathrm{d}t}\left(\varepsilon \Delta_\perp \phi - \mathbf{B}_{||}\right) = 0 \;,$$

except for inclusion of the last equation and a small term with $\mathbf{B}_{||}$ in the operator:

$$\frac{\mathrm{d}}{\mathrm{d}z} = \frac{\partial}{\partial z} + \mathbf{B}_{||}\frac{\partial}{\partial z} - \{\mathbf{A}, ...\} \;.$$

The Eq. (3) was derived in the lowest approximation on the small parameter. The partial solutions of the system are both vortices and nonlinear localized solutions. The latter solutions are typical feature of the equations with the Korteweg – de Vries nonlinearity, which deals with compression effects.

Partial solution: vortex-type structure

Drift Alfven vortices are obtained by taking into account the vector-type nonlinearity of the Poisson brackets and by neglecting the compression. A partial solution was obtained in a number of papers (Chmyrev et al., 1988; Petviashvili and Pokhotelov, 1989) and took
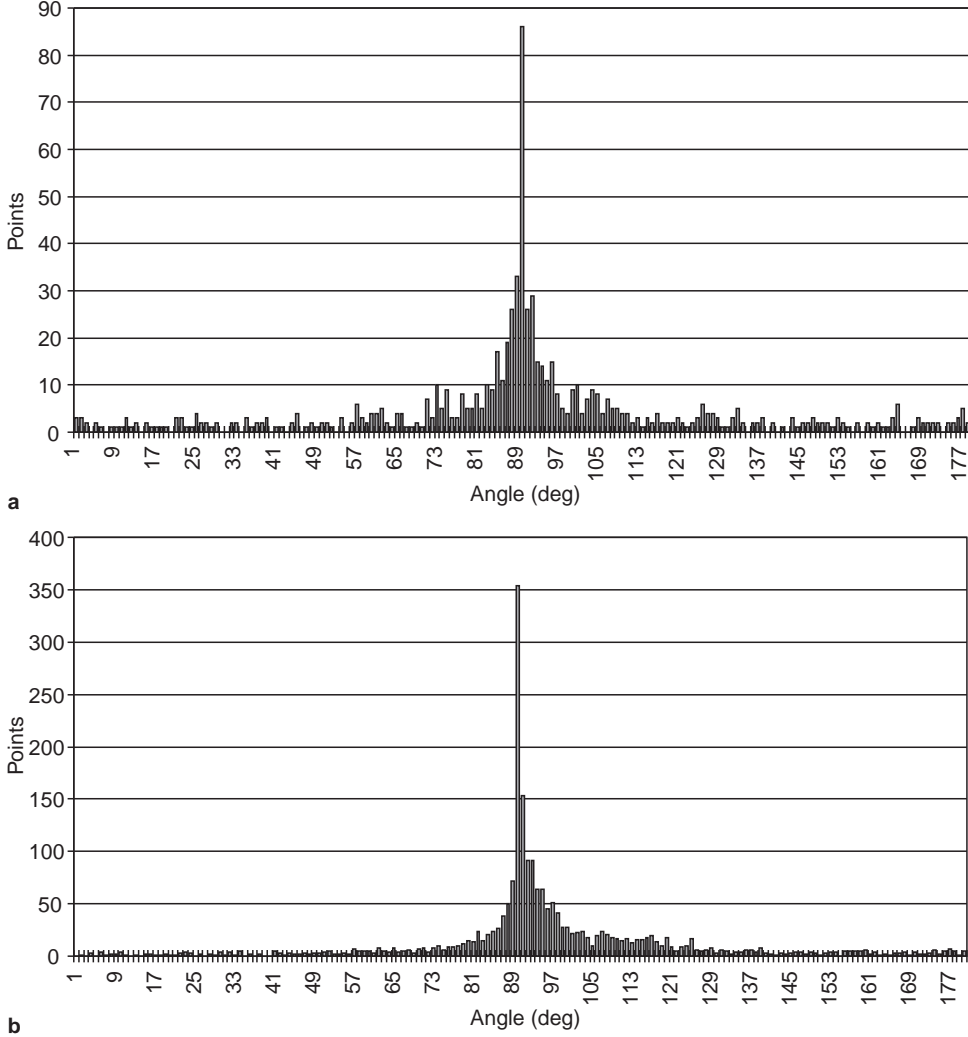
a

b

Fig. 7a, b. Distribution of the measurements made in **a** October 1995 and **b** October 1996 versus angle between the local magnetic field line and the flow velocity vector

the form of a dipolar vortex in the polar coordinates in a definite plane:

$$\mathbf{A} = [\alpha\,\mathbf{r} + C_1\mathbf{J}_1(\mathbf{k}_1\mathbf{r}) + C_2\mathbf{J}_2(\mathbf{k}_2\mathbf{r})]\cos\theta, \quad \mathbf{r} \leq \mathbf{r}_0,$$
$$\mathbf{A} = C_3\mathbf{k}_1(\mathbf{sr})\cos\theta, \quad \mathbf{r} \geq \mathbf{r}_0 \ . \tag{4}$$

Here $\alpha, \mathbf{k}_1, \mathbf{k}_2, \mathbf{s}$ and $\mathbf{r}_0$ are parameters of the solution. This vortex is a localized structure and exponentially decreases at large distances from its centre. This solution represents vortical flows in a plane. However, we neglect magnetic field disturbances along the field line and compressional effects which are important for the wave events under study.

Partial solution: soliton-type structure

Axisymmetric partial solution of the system (3) in a plane $(\mathbf{r}, \eta)$, where

$$\mathbf{r} = \sqrt{x^2 + y^2}, \quad \eta = y - ut + \alpha z, \quad \alpha = \arctan(\eta/x) \ ,$$

can be constructed by standard methods (e.g. see Petviashvili and Pokhotelov, 1989; Chmyrev *et al.*, 1988). Axisymmetric drift Alfven vortex obeys the equation:

$$\Delta_\perp\mathbf{A} - \mathbf{s}^2\mathbf{A} = \varepsilon\frac{\alpha^3}{u(\delta u^2 - \alpha^2)}\Delta_\perp\mathbf{A}\frac{\partial}{\partial r}(\Delta_\perp\mathbf{A} - \mathbf{A}) \ , \tag{5}$$

which differs from the results of Chmyrev *et al.* (1988) by the small term proportional to ε. Here, **s** is a parameter. By iterating we can construct the following equation:

$$\Delta_\perp\mathbf{A} - \mathbf{s}^2\mathbf{A} - q\,\mathbf{A}^2 = 0, \quad q = \varepsilon\frac{\alpha^3(1-\delta)(u^2-\alpha^2)}{2} \ .$$

An equation of the same form was studied numerically (Horton and Hasegawa, 1994). Its solution is:

$$A \approx -\frac{2.4\mathbf{s}^2}{q} \cdot \left(\mathrm{sec}\,\mathrm{h}\frac{3\mathbf{s}\,\mathbf{r}}{4}\right)^{4/3} \ , \tag{6}$$

which describes soliton-like impulses of the potential. Particle number density also has a solution in the form of Eq. (6). This effect is possibly the result of plasma trapping in the nonlinear wave structure.

A compressional effect producing in a warm plasma results in small variations along the field line $(\mathbf{B}_\| \neq 0)$ and soliton-like axisymmetric structures. This effect deals with solitons which are common for nonlinear magnetosonic waves. It should be noted that variations
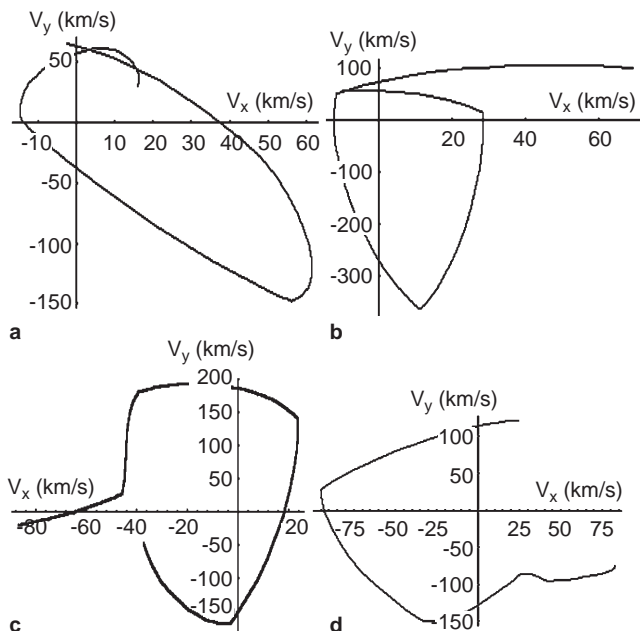
Fig. 8a–d. Hodographs of the plasma flow velocity (km/s) in the GSM coordinates for the selected time intervals with the dissimilarities in pressure time series: **a** 11:55 – 12:05 2 October, 1995; **b** 04:40 – 04:50 25 October, 1995; **c** 18:22 – 18:34 3 October, 1996; **d** 06:44 – 06:54 23 October, 1996
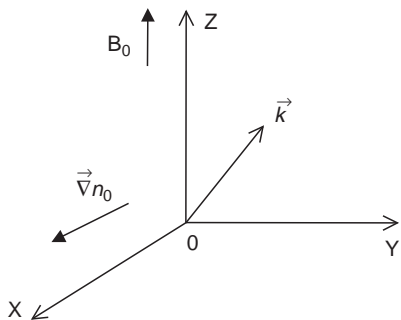

Fig. 9. The plasma system model

of the parallel magnetic field are also connected with the vorticity of the plasma by the expression:

$$\mathbf{B}_{\parallel} \approx \varepsilon \Delta_{\perp} \phi = \varepsilon \Omega, \quad \Omega = \left[\vec{\mathbf{V}}_{\perp}, \vec{\mathbf{V}}_{\perp} \right] ,$$

which provides the vortex solutions.

Conclusions

We have analyzed magnetic field and plasma data obtained with Interball-1 in the low-latitude dawn flank of the magnetosphere. The study was made in the middle tail at radial distances of about 10–20 R_E. Compressional Pc-5 type disturbances were found in the dawn plasma sheet. By searching for morphological similarities it is possible to select time intervals with distinct anti-phase variations of the magnetic and plasma pressures. The model estimation of wave struc-

ture was made by averaging the magnetic field data over 1 h time intervals.

From the results obtained several conclusions can be made:

1. Compressional large-scale waves were detected in the dawn flank of the middle tail. Preliminary results show that these events are absent in the dusk flank. Possible dawn-dusk asymmetry in excitation of the compressional waves in the low-latitude plasma sheet requires further study.
2. These wave events represent features of both Alfven waves and magnetosonic waves. Variations of compressional and transverse magnetic field components are of the same order of magnitude.
3. Vortices were found at the time intervals under study. Plasma rotation occurs predominantly in the orthogonal direction to the local field line. Due to the field line curvature, there is no fixed position of rotational plane in a space.
4. Theoretical model of the listed processes taking into account the coupling of drift Alfven and magnetosonic waves is proposed. A vortex is the partial solution of the set of the equations when compression is neglected. The compression effect gives raise to nonlinear soliton-like solution.

Successive approximations of the small parameter ε will provide the theoretical model with input on the compressional effects. This is the subject of further study. Thus the partial solution of the system (3) representing both vortex and compressional properties will be obtained.

Further progress in the problem of compressional large-scale events is connected with multipoint measurements of the magnetic field structure and velocity fields. It seems promising to make comparison with the Geotail measurements of ULF wave events made in the tail.

References

Anderson B. J., Engebretson, M. J., Rounds, S. P., Zanetti, L. J., and Potemra, T. A., A statistical study of Pc3–5 pulsations observed by the AMPTE/CCE magnetic field experiment. 1. Occurrence distributions, *J. Geophys. Res.*, **95**(A7)**,** 10 495–10 523, 1990.

Barfield, J. N. and Lin, C. S., Remote determination of the outer radial limit of stormtime Pc5 wave occurrence using geosynchronous satellites, *Geophys. Res. Lett.*, **10,** 671, 1983.

Barfield, J. N., and McPerron, R. L., Storm time Pc5 magnetic pulsations observed at synchronous orbit and their correlation with the partial ring current, *J. Geophys. Res.*, **83**, 739, 1978.

Basseville, M., and Beveniste, A., (Eds.), *Detection of abrupt changes in signals and dynamical systems*, Springer-Verlag, Berllin Heidelberg New York, 1986.

Bauer, T. M., Baumjohann W., Treumann R. A., and Sckopke N., Low-frequency waves in the near-Earth plasma sheet, *J. Geophys. Res.*, **100**(A6), 9605–9617, 1995.

Chan, A. A., Xia, M., and Chen, L., Anisotropic Alfven-ballooning modes in Earth's magnetosphere, *J. Geophys. Res.*, **99**(A9), 17 351–17 366, 1994.

Chen, L., and Hasegawa, A., Kinetic theory of geomagnetic pulsations. 1. Internal excitations by geomagnetic particles, *J. Geophys. Res.*, **96**(A2), 1503–1512, 1991.

Chen, L., and Hasegawa, A., Kinetic theory of geomagnetic pulsations. 2. Ion flux mudulations by transverse waves, *J. Geophys. Res.*, **99**(A1), 179–182, 1994.

Cheng, C. Z., A kinetic magnetohydrodynamic model for low-frequency phenomena, *J. Geophys. Res.*, **96**(A12), 21 159–21 171, 1991.

Cheng, C. Z., and Qian, Q., Theory of ballooning-mirror instabilities for anisotropic pressure plasmas in the magnetosphere, *J. Geophys. Res.*, **99**(A6), 11 193–11 209, 1994a.

Cheng, C. Z., Qian, Q., Takahashi, K., and Lui, A. T. Y., Ballooning-mirror instability and internally driven Pc4–5 wave events, *J. Geomag. Geoelectr.*, **46**, 997–1009, 1994b.

Chmyrev, V. M., Bilichenko, S. V., Pokhotelov, O. A. et al., Alfven vortices and related phenomena in the ionosphere and the magnetosphere, *Phys. Scripta*, **38**, 841, 1988.

Christon, S. P., Eastman, T. E., Doke, T. et al., Magnetospheric plasma regimes using Geotail measurements, 2. Statistics, spatial distribution, and geomagnetic dependence, *J. Geophys. Res.*, **103**, 23 521–23 542, 1998.

Eastman, T. E., Christon, S. P., Doke, T. et al., Magnetospheric plasma regimes using Geotail measurements, 1. Regime identification and distant tail variability, *J. Geophys. Res.*, **103**, 23 503–23 520, 1998.

Hones, E. W., Jr., Paschmann, G., Bame, S. J. et al., Vortices in magnetospheric plasma flow, *Geophys. Res. Lett*, **5**(12), 1059–1062, 1978.

Hones, E. W., Jr., Birn, J., Bame, S. J. et al., Further determination of the characteristics of magnetospheric plasma vortices with ISEE 1 and 2, *J. Geophys. Res.*, **86**(A2), 814–820, 1981.

Hones, E. W., Jr., Birn, J., Bame, S. J., and Russell, C. T., New observations of plasma vortices and insights into their interpretation, *Geophys. Res. Lett*, **10**(8), 674–677, 1983.

Horton, W., and Hasegawa, A., Quasi-two-dimensional dynamics of plasma and fluids, *Chaos*, **4**(2), 227–251, 1994.

Huang, X., and Miller, W., A time-efficient, linear-space local similarity algorithm, *Adv. Appl. Math.*, **12**, 337–357, 1991.

Huang, X., and Waterman M. S., Dynamic programming algorithms for restriction map comparison, *CABIOS*, **8**(5), 511–520, 1992.

Klimov, S., Romanov, S., Amata, E., Blecki, J., Buechner, J., Juchniewicz, J., Rustenbach, J., Triska, P., Woolliscroft, L. J. C., Savin, S., Afanas'yev, Yu., deAngelis, U., Auster, U., Bellucci, G., Best, A., Farnik, F., Formisano, V., Gough, P., Grard, R., Grushin, V., Haerendel, G., Ivchenko, V., Korepanov, V., Lehmann, H., Nikutowski, B., Nozdrachev, M., Orsini, S., Parrot, M., Petrukovich, A., Rauch, J. L., Sauer, K., Skalsky, A., Slominski, J., Trotignon, J. G., Vojta, J., and Wronovski, R., ASPI experiment: measurements of fields and waves onboard the INTERBALL-1 spacecraft, *Ann. Geophysicae.*, **15**, 514–527, 1997.

Kokubun, S., Kivelson, M. G., McPerron, R. L., Russell, C. T., and West, H. J., OGO 5 observations of the Pc5 waves: particle flux modulations, *J. Geophys. Res.*, **82**, 2774, 1977.

Mikhaylovskiy, A. B., *Electromagnetic instabilities of in-homogeheous plasma*, Nauka Publishing House, Moscow, 1991.

Petviashvili, V. I., and Pokhotelov, O. A., *Soviet Physics – JETP Lett.*, **42**, 54, 1985.

Petviashvili, V. I., and Pokhotelov, O. A., *Solitary waves in plasma and atmosphere*, Nauka Publishing House, Moscow, 1989.

Saunders, M. A., Southwood, D. J., Hones, E. W., Jr., and Russell, C. T., A hydromagnetic vortex seen by ISEE-1 and 2, *J Atmos. Terr. Phys.*, **43**(9), 927–932, 1981.

Saunders, M. A., Southwood, D. J., Fritz, T. A., and Hones, E. W. Jr., Hydromagnetic vortices-I. The 11 December 1977 event, *Planet. Space Sci.*, **31**(10), 1099–1115, 1983a.

Saunders, M. A., Southwood, D. J., and Hones, E. W., Jr., Hydromagnetic vortices-II. Further dawnside events, *Planet. Space Sci.*, **31**(10), 1117–1127, 1983b.

Sibeck, D. G., Lopez, R. E., and Roelof, E. C., Solar wind control of the magnetopause shape, location and motion, *J. Geophys. Res.*, **96**(A4), 5489–5495, 1991.

Su, S.-Y., Konradi, A., and Fritz, T. A., On propagation direction of ring current proton ULF waves observed by ATS 6 at 6.6 Re, *J. Geophys. Res.*, **82**(A3), 1859–1867, 1977.

Takahashi, K., Higbie, P. R., and Baker, D. N., Azimuthal propagation and frequency characteristics of compressional Pc 5 waves observed at geostationary orbit, *J. Geophys. Res.*, **90**(A2), 1473–1485, 1985.

Takahashi, K., Fennell, J. F., Amata, E., and Higbie, P. R., Field-aligned structure of the storm time Pc5 wave of November 14–15, 1979, *J. Geophys. Res.*, **92**, 5857, 1987.

Takahashi, K., Multisatellite studies of ULF waves, *Adv. Space Res.*, **8**(9–10), 9427–9436, 1988.

Takahashi, K., Cheng, C. Z., McEntire, R. W., and Kistler, L. M., Observation and theory of Pc5 waves with harmonically related transverse and compressional components, *J. Geophys. Res.*, **95**(A2), 977–989, 1990.

Tsyganenko, N. A., Modeling the Earth's magnetospheric magnetic field confined within a realistic magnetopause, *J. Geophys. Res.*, **100**(A4), 5599–5612, 1995.

Tsyganenko, N. A., and Stern, D. P., A new-generation global magnetosphere field model, based on spacecraft magnetometer data, *ISTP Newsle.*, **6**(1), 21, 1996.

Walker A. D. M., Greenwald, R. A., Korth A., and Kremser, G. Stare and GOES2 observations of a storm time Pc5 ULF pulsations, *J. Geophys. Res.*, **87**, 9135–9146, 1982.

Yermolaev Y. I., Fedorov, A. O., Vaisberg, O. L., Balebanov, V. M., Obod, Y. A., Jimenez, R., Fleites, J., Llera L., and Omelchenko, N. A., Ion distribution dynamics near the Earth's bow shock: first measurements with the 2D ion energy spectrometer CORALL on the INTERBALL/Tail-probe satellite, *Ann. Geophysicae*, **15**, 533–541, 1982.

Zhu, X., and Kivelson, M. G., Compressional waves in the outer magnetosphere. 1. Statistical study, *J. Geophys. Res.*, **96**(A11), 19 451–19 467, 1991.

Zhu, X., and Kivelson, M. G., Compressional ULF waves in the outer magnetosphere: 2. A case study of Pc5 type activity, *J. Geophys. Res.*, **99**(A1), 241–252, 1994.